

A six hundred-year annual minimum temperature history for the central Tibetan Plateau derived from tree-ring width series

Minhui He · Bao Yang · Nina M. Datsenko

Received: 22 March 2013 / Accepted: 15 July 2013 / Published online: 31 July 2013
© Springer-Verlag Berlin Heidelberg 2013

Abstract The recent unprecedented warming found in different regions has aroused much attention in the past years. How temperature has really changed on the Tibetan Plateau (TP) remains unknown since very limited high-resolution temperature series can be found over this region, where large areas of snow and ice exist. Herein, we develop two *Juniperus tibetica* Kom. tree-ring width chronologies from different elevations. We found that the two tree-ring series only share high-frequency variability. Correlation, response function and partial correlation analysis indicate that prior year annual (January–December) minimum temperature is most responsible for the higher belt juniper radial growth, while more or less precipitation signal is contained by the tree-ring width chronology at the lower belt and is thus excluded from further analysis. The tree growth-climate model accounted for 40 % of the total variance in actual temperature during the common period 1957–2010. The detected temperature signal is further robustly verified by other results. Consequently, a six century long annual minimum temperature history was firstly recovered for the Yushu region, central TP. Interestingly, the rapid warming trend during the past five decades is identified as a significant cold phase in the context of the past 600 years. The recovered temperature series reflects low-frequency variability consistent with

other temperature reconstructions over the whole TP region. Furthermore, the present recovered temperature series is associated with the Asian monsoon strength on decadal to multidecadal scales over the past 600 years.

Keywords Tree rings · Temperature variation · Tibetan Plateau · Climate of the past

1 Introduction

Global warming and associated regional climatic changes have attracted much attention in recent years. Examples include the influence of the warming trend on tree structure, position and the ecosystem (Harsch et al. 2009; Liang et al. 2011; Zhang et al. 2011). Statistically significant overall warming trends have been found over the Tibetan Plateau (TP) during recent decades (Yang 2012), especially at high elevation sites (Liu and Chen 2000). In the central region, for example, as calculated from Qumalai meteorological station data, annual (January–December) temperature, maximum temperature and minimum temperature all showed increasing trend during the past five decades, with increasing slopes of 0.68, 0.69 and 0.46, respectively. These results indicate that the regional climate has changed thoroughly within the past 50 years. Nonetheless, to interpret such a significant warming trend from a longer-term perspective and/or to test whether these changes are still within the range of natural climate variability, we need to extract information from proxy data, since the relatively small spatial coverage and short records of the available meteorological stations limit our understanding. Such proxy data can be extracted from various natural archives, such as historical records, tree rings, ice cores, lake or marine sediments, and so on (for a review, see Jones et al. 2009).

M. He · B. Yang (✉)
Key Laboratory of Desert and Desertification, Cold and Arid Regions Environmental and Engineering Research Institute, Chinese Academy of Sciences, 320 Donggang West Road, Lanzhou 730000, China
e-mail: yangbao@lzb.ac.cn

N. M. Datsenko
Hydrometeorological Research Centre of Russia, Bolshoy Predtechensky lane 9/11, 123242 Moscow, Russia

Long, annually resolved tree-ring records have been used to investigate large-scale spatiotemporal climate change during the past decades (e.g., Briffa 2000; Briffa et al. 2002, 2004; Luterbacher et al. 2004; Büntgen et al. 2005, 2006, 2011; D'Arrigo et al. 2006; Mann et al. 2009; Cook et al. 2010; Yang et al. 2012a, b). Tibetan juniper (*Sabina tibetica* Kom.) is notable for its individual longevity. Long-lived juniper trees can reach ages of thousands of years, and the annually resolved ring-width chronologies make the proxy a rare and valuable resource in paleoclimatology. Specifically, for the central TP region, where contains large areas of ice cores and probably falls in the transect of the different precipitation trends over southern and northern TP (Wang et al. 2007), however, very limited longer-term and high-resolution climate records can be found (Jin et al. 2005; Xu et al. 2011; Zhu et al. 2011; Wang et al. 2013). Consequently, there is an obvious necessity for additional data collection from regular network sources to explore the corresponding climate changes in this area.

The objectives of this study are to (1) develop new tree-ring width chronologies for the central TP region, (2) identify the most responsible climate for tree radial growth, (3) reconstruct past climate changes using well calibrated and verified tree growth-climate relationships, (4) overview recent climatic change in a longer term context, and (5) evaluate the linkage between regional climate and large-scale spatial temperature variability.

2 Materials and methods

2.1 Study area and climate

Our study area is located in the Yushu region, central TP (Fig. 1), where the climate is mostly affected by the South Asian summer monsoon. Records from the nearest meteorological station Qumalai (34.13°N, 95.75°E, 4,175 m a.s.l.) show that mean annual temperature is about -2.1 °C from 1957 to 2010, with July (mean temperature of 8.9 °C) and January (-13.8 °C) being the warmest and the coldest month, respectively (Fig. 2). Local mean annual precipitation is about 409 mm, the majority (87.9 %) of which falls during May–September. The region is characterized by a cold and arid plateau climate. Compared to the typical arid Qilian mountain region (e.g., recorded from Jiuquan station, local mean annual temperature is about 7.48 °C, with July of 21.98 °C and January of -9.43 °C, mean annual precipitation is about 87 mm), we consider that the present one is more cold and humid, so local tree growth may bear an important imprint of the temperature signal.

2.2 Tree-ring sampling and chronology development

We used two sampling sites, Qumalai (QML, 33.8°N, 96.2°E) and Zhiduo (ZHD, 33.7°N, 96.3°E), about 30 km apart. Their ecological settings are very homogenous. The openness of the forest stands ensures that tree-ring series are virtually free from stand dynamics effects, and maximizes the chance for retaining common forcing of tree growth by climate. Hence, mature trees free from obvious disease or human activities were selected for sampling. One or two cores per tree from different directions were collected at breast height with increment borers. Trees were sampled along an altitudinal range of 3,975–4,370 m a.s.l. on the mountainous slopes. In total, 82 (32) cores from 49 (20) trees were sampled at the QML (ZHD) “lower-altitude” forest belt (3,975–4,145 m); 77 (22) cores from 45 (17) trees were sampled at the QML (ZHD) “higher altitude” forest belt (4,160–4,370 m). The median heights of the two sub-elevation belts are 4,014 and 4,217 m, respectively. The relevant 25 and 75 percentile heights for the lower (higher) elevation are 3,997 m (4,193 m) and 4,061 m (4,293 m), respectively.

All tree-ring samples were processed following standard dendrochronological practice (Stokes and Smiley 1968). Ring width was recorded by the measuring system LINTAB with a resolution of 0.01 mm, and all cores were cross-dated by pattern matching and statistical tests in the software package TSAP (Rinn 2003). The quality of the cross-dating was checked using the COFECHA program, which can ensure exact dating for annual ring width by correcting the potential bias of missing rings and dating errors (Holmes 1983). The final chronology was developed with the ARSTAN program (Cook 1985). Prior to standardization, a data adaptive power transformation was applied to reduce the potential heteroscedasticity commonly found in the raw ring-width measurements (Cook and Peters 1997). To remove the influences of age or other factors unrelated to climate, the raw series were detrended conservatively using either a linear or negative exponential function. A cubic smoothing spline with a frequency cut-off equal to two-thirds of the series length was further used in a few cases when anomalous growth trends occurred. Tree-ring indices were then calculated as the residuals between the measured ring width and the corresponding value of the fitted curve. This method avoids possible “end-effect” bias in the resulting tree-ring chronologies due to index inflation after calculating ratios (Cook and Peters 1997). The detrended tree-ring series were averaged to a standard site chronology using a biweight robust estimate of the mean to minimize the influence of outliers (Cook and Kairiukstis 1990). To reduce the effect of higher standard deviations in weakly replicated portions of the

Fig. 1 Locations of the studied tree-ring sampling sites (QML and ZHD), 63 meteorological stations on the Tibetan Plateau and other investigated sites mentioned in the text. *A*, the tree-ring sites in this study; *B*, the Qamdo site in Yang (2012); *C*, the study area in Cook et al. (2003)

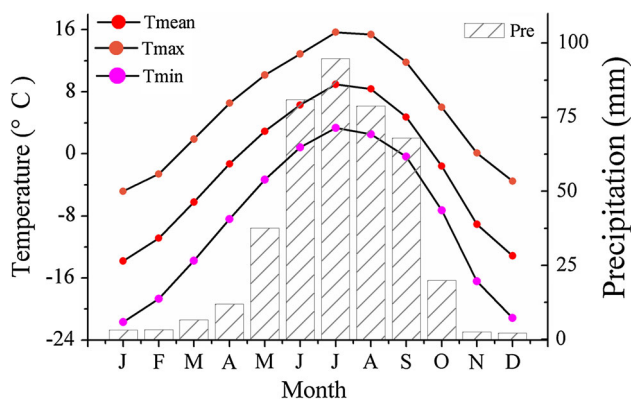
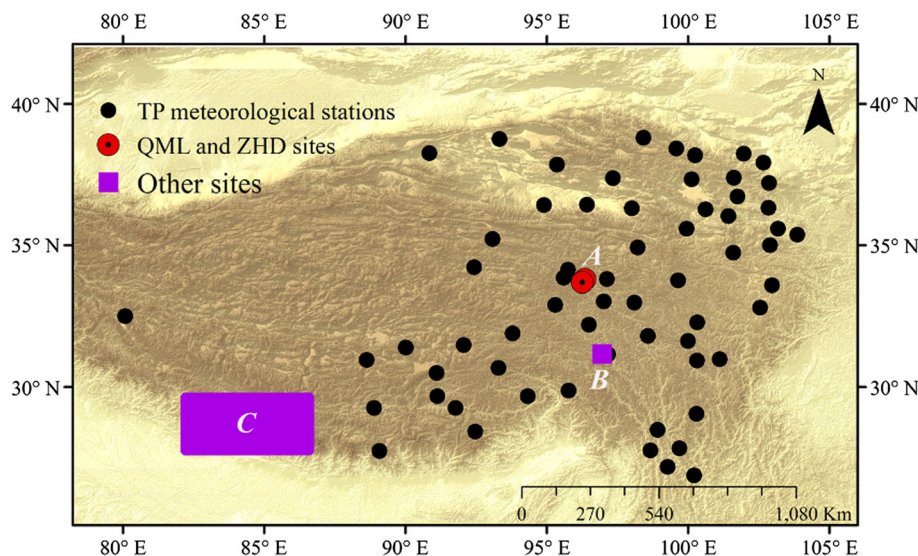


Fig. 2 Climate conditions (monthly mean temperature, monthly mean minimum temperature, monthly mean maximum temperature and monthly precipitation amount) inferred from Qumalai station (1957–2010) in the study region

chronology, the variance was stabilized following the method described by Osborn et al. (1997). The expressed population signal (EPS) (Wigley et al. 1984), which was calculated in a 30-year running window with 15-year overlaps and was considered to provide an absolute measure of signal quality through time (Briffa 1995), was used with a threshold value of 0.85 to determine the reliable period of the chronologies. Hence, at the higher forest belt, QML and ZHD chronologies give the reliable period of AD 1440–2010 and AD 1585–1945, respectively, while at the lower belt, the two chronologies exhibit reliable period of AD 1660–2010 and AD 1495–1945. The statistical confidence of the chronology was assessed using bootstrapped error bars (Efron 1987).

The raw and standard chronologies at the two belts for the common reliable periods AD 1585–1945 and 1660–1945 were compared for coherence using correlation analysis. These chronologies showed very high correlations

($r_{\text{raw}} = 0.71$ and $r_{\text{std}} = 0.73$ for the higher belt; $r_{\text{raw}} = 0.62$ and $r_{\text{std}} = 0.58$ for the lower belt) despite the comparatively low sample replication in the ZHD chronology, indicating a strong regional climate signal. Thereafter, we combined all the relevant raw tree-ring width data from the two sites to develop longer and better replicated regional “higher” and “lower” ring-width composite chronologies. They were developed based on the methods described above.

2.3 Statistical analysis

To compare the similarities and differences between the higher and lower altitudinal chronologies, we performed high-pass and low-pass filtering on the raw standard tree-ring chronologies over the common reliable period. Correlation calculation of the original unfiltered data, the high-pass filtered data and the low-pass filtered data was performed. Since there are strong autocorrelations in the low-pass filtered data, the degree of freedom for significance testing was adjusted with the method described by Bretherton et al. (1999). The variability of the two chronologies in the frequency domain was examined using the multi-taper method (MTM) of spectral analysis (Mann and Lees 1996).

Tree growth-climate relationships between standard chronology and regional climate factors (monthly mean temperature, monthly minimum temperature, monthly maximum temperature and monthly total precipitation) were determined using correlation and response analyses in the DendroClim 2002 program (Biondi and Waikul 2004). The correlations were calculated on a 24-month period beginning in January of the prior growth year to December of the growth year. This “climate window” allows the assessment of the influence of previous and present year’s

climate on current year's growth. Correlations were also calculated between tree-ring series and climate data over various multi-month seasons or a full-year scale. Furthermore, partial correlations were calculated to determine the specific climatic factors most strongly associated with local tree growth.

A transfer function was estimated by linear regression using the appropriate climate data as the dependent variable and tree-ring chronology as the independent variable. To test the validity of our climate–growth model, we used split sample calibration–verification tests (Meko and Graybill 1995). The reliability of the regression model was also evaluated by employing the leave–one–out cross verification method (Michaelsen 1987). In the leave–one–out validation, each value was removed once from observed temperature series and predicted by a model generated from the remaining data. Moreover, sign test (ST) and product mean test (Pmt) statistics were applied (Fritts 1976). The ST counts the number of agreements and disagreements between the reconstructed and the instrumental climate data, while Pmt measures the level of agreement between the actual and estimated values and takes into account the sign and magnitude of departures from the calibration average. In order to validate the reconstruction, it was further compared with other related temperature series both on regional and large-scale variability.

3 Results

3.1 Characteristics of the tree-ring chronology

The compared features of the tree-ring standard chronologies at the higher and lower belts are shown in Fig. 3 and Table 1. The mean segment length (MSL) as well as the 25, 50 and 75 percentile age (265, 389 and 536) of the higher chronology are longer than the relevant lower chronology (214, 288 and 401). Since Cook et al. (1995) stated that the lowest frequency of climate information that can be realistically recovered from traditionally standardized series is $3/n$ cycles per year (where n is the MSL), both the two chronologies have the ability to resolve interdecadal to multidecadal scale tree growth variations that are likely related to climate change. The mean sensitivity, which is a measure of relative difference in ring widths between adjacent rings, is higher than that in the central Hengduan Mountains (Li et al. 2012). The high first-order autocorrelation (AC1) of the two chronologies is considered to be biological in origin (Fritts 1976). The higher and lower belts' tree-ring standard chronologies covered the reliable periods AD 1395–2010 and AD 1480–2010, based on the arbitrary EPS cutoff value of 0.85 (Wigley et al. 1984). Compared to the lower forest belt chronology, the

higher belt chronology exhibits higher values of the variance explained by the first principal component (PC#1), signal to noise ratio (SNR), EPS and average correlation among the individual tree-ring series. Overall, the relatively higher values of all the statistics imply that more climatic signals are contained by the two altitudinal tree-ring chronologies and they can be used as promising proxies for climate change studies.

3.2 Comparison of the two altitudinal chronologies

The significant ($p = 0.01$) correlation ($r = 0.68$) between the two original chronologies over the common reliable period AD 1480–2010 seemingly implies that the two series are probably driven by the same climatic signal. However, when we decomposed the original chronology into high- and low-pass filtered series, the relevant correlations are 0.86 (significant at the 0.001 level) and 0.51. Considering the degree of freedom for significance testing described by Bretherton et al. (1999), the correlation of the 0.51 for the low-frequency variability is not statistically significant at the 0.05 level. Besides, the correlation coefficient between the first-order difference series of the two original chronologies is 0.85 (significant at the 0.001 level). Hence, we state that the two altitudinal chronologies only share high-frequency variability, but not low-frequency variability, as also presented in Fig. 3 of the 11-year smoothed series for the two chronologies. Such results were also verified by the MTM analysis (Fig. 4) for the two original chronologies over their common reliable period. Although the two chronologies hold the same significant (95 % confidence level) $\sim 80a$ cycle, only the lower belt chronology exhibits the significant $\sim 44a$ cycle at the detected low-frequency variability. The robust common high-frequency variability of $\sim 2a$ oscillation was defined by the two series. Overall, the above mentioned comparisons give evidence for the inconsistent variability of the two chronologies over their reliable period. Consequently, it seems unsuitable to combine both the higher and lower chronologies to develop a longer composite chronology in the study region.

3.3 Tree growth–climate relationships at the two altitudinal forest belts

How climate directly drives the two tree-ring width series was evaluated by the associations with the available climate data. Results of tree growth–climate relationships (Fig. 5a) show a general positive correlation between local juniper radial growth and mean temperature (T_{mean}) of all months except for current May ($r = -0.07$) at the higher forest belt and for April ($r = -0.04$) and May ($r = -0.08$) at the lower belt. Significant ($p = 0.05$) correlation and

Fig. 3 Characteristics of the two altitudinal standard chronologies (blue line) and the 11-year Fast Fourier Transformed (FFT) series (red heavy line) with the corresponding EPS (red lines), Rbar (gray lines) and sample depth (gray area). The dashed red line shows the EPS = 0.85 cut-off. The rectangles with gray oblique lines indicate the less reliable periods for the individual standard chronology

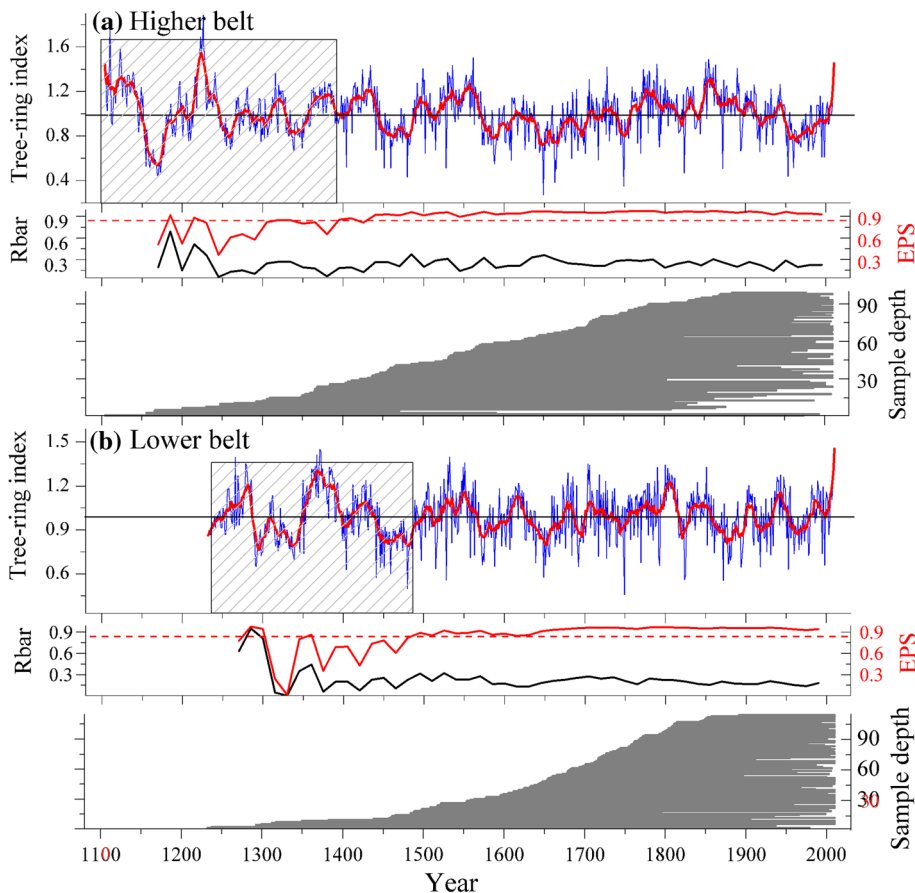


Table 1 General characteristics of the two standard chronologies

Time span	Lower belt 1232–2010	Higher belt 1104–2010
Cores/trees	114/69	99/62
MSL	324	404
SD	0.17	0.21
MS	0.14	0.15
AC1	0.42	0.56
PC#1	17.00	24.05
SNR	22.99	37.53
EPS	0.96	0.97
EPS > 0.85	1480/11	1395/8
R1	0.33	0.39
R2	0.67	0.66
R3	0.33	0.39

MSL is the mean segment length; SD is the standard deviation; MS is the mean sensitivity; AC1 is the first order autocorrelation; PC#1 is the variance explained by the first principal component; SNR is the signal-to-noise ratio; EPS is the expressed population signal; EPS > 0.85 indicates the year and number of trees with expressed signal strength above 0.85; R1 is the all series Rbar; R2 is the within trees Rbar; R3 is the among trees Rbar

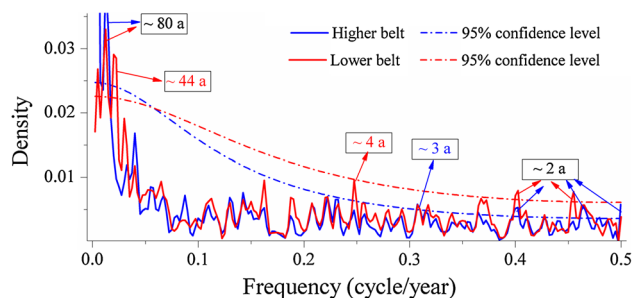
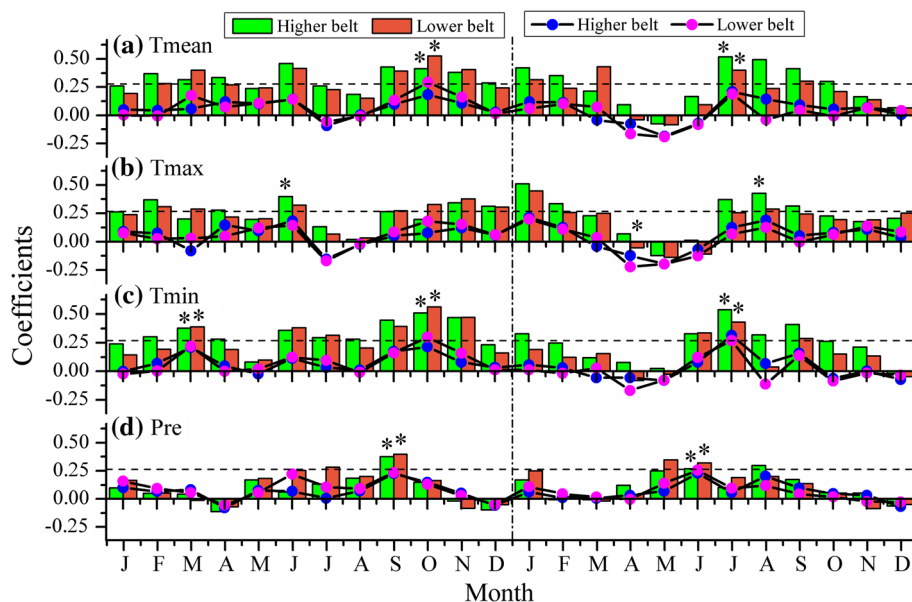


Fig. 4 Multi-taper method (MTM) spectral density of the two tree-ring width chronologies over the common reliable period AD 1480–2010. The dash-dotted lines indicate the 95 % confidence levels for the two series

response function with T_{mean} occur in prior October and current July at the two elevation belts. Previous June ($r = 0.40$) and current August ($r = 0.43$) maximum temperature (T_{max} , Fig. 5b) significantly ($p = 0.05$) influence tree growth at the higher forest belt. No significant ($p = 0.05$) positive correlation between monthly T_{max} and tree-ring series was found at the lower elevation belt, and inversely, a significant negative response function was

Fig. 5 Correlations (*histogram bars*) and response functions (*lines with circles*) between the two standard tree-ring chronologies and monthly **a** mean temperature (T_{mean}), **b** maximum temperature (T_{max}), **c** minimum temperature (T_{min}) and **d** precipitation (Pre) from prior January to current December over the common period 1957–2010. The *horizontal dashed lines* indicate the 95 % confidence level for the correlation function. Response functions significant at 0.05 levels are marked with an *asterisk*



detected from current April. Previous March and October as well as current July minimum temperature (T_{min} , Fig. 5c) all show significant ($p = 0.05$) correlations and response values with tree-ring series at the two forest belts. Herein, all the months' temperatures (T_{mean} , T_{max} and T_{min}) in the previous year hold consistent positive correlations with tree-ring series at both the higher and lower elevation belts.

The associations between monthly precipitation (Fig. 5d) and tree-ring series are weaker, with the highest and also significant ($p = 0.05$) positive correlations in prior September at the higher ($r = 0.37$) and lower ($r = 0.39$) altitudinal belts. Current June precipitation also significantly promotes all the sampled radial tree growth. Prior June, July and current January precipitation exhibit significant correlations with the lower belt radial tree growth, but the corresponding response functions do not reach the 0.05 significance level.

We also calculated correlations between tree-ring series and seasonally or annually averaged climatic variables to examine the accumulative effects of climate variables on tree growth. Again, the corresponding correlations of the first-order (1st) difference series and the 5-year smoothed series were further analyzed to investigate whether the associations are robust both at the high- and low-frequency variability over the common period 1957–2010. All the presented results in Table 2 indicate that the associations between tree-ring series at the lower elevation belt and the colder season (previous September to current March: $T_{\text{mean}} = -7.2$ °C; $T_{\text{max}} = 1.2$ °C; $T_{\text{min}} = -8.7$ °C) temperatures are a little weaker than, or at most equal to, that at the higher belt. The negative effect of maximum temperature on both the two tree-ring series do not reach the 0.05

significance level during April–May before the arrival of the main Asian monsoon season. However, compared to juniper growth at the higher elevation belt, the lower altitudinal tree-ring width may benefit from more seasonal (May–September, c_5 – c_9) or annual (previous July to current June, p_7 – c_6) precipitation. Considering all the listed associations together, we speculate that the higher altitudinal tree-ring chronology contains more temperature signal, while the lower belt tree-ring chronology may include both temperature and precipitation signals. Such speculations were verified by the partial correlation analysis. For the higher altitudinal tree-ring series, when controlling for the annual minimum temperature, correlations with precipitation do not reach the significance level ($p < 0.001$); when controlling for precipitation, correlations with the annual minimum temperature are significant. However, for the lower elevation chronology, all the associated correlation coefficients fail to reach the significance level, no matter which climatic parameter is controlled. Hence, samples from the lower belt are excluded from further analysis since they may introduce unwanted signals of precipitation variations. The higher altitudinal chronology shows significant (0.05 level) correlations (0.38–0.64) with annual minimum temperature (p_{1-12} , p_{10-C9} , p_9-C8 , p_8-C7 , p_7-C6) both in the original and the first-order difference series, indicating that local tree-ring records contain strong annual minimum temperature signals. To preserve as many of the climate footprints as possible in both the high- and low-frequency variability, it is reasonable for us to select the previous mean annual minimum temperature for the reconstruction. This proxy yields the highest correlations between the corresponding original series and the first-order difference series, as well as the 5-year smoothed

Table 2 Correlation coefficients between the higher (lower) elevation tree-ring series and seasonal assembled or annual climate data during the common period 1957–2010

	Original series	1st difference series	5-year smoothed series
P ₉ -C ₃ T _{mean}	0.56** (0.52**)	0.34* (0.34*)	0.83 (0.62)
P ₁₀ -C ₉ T _{mean}	0.56** (0.45**)	0.26 (0.17)	0.86 (0.74)
P ₉ -C ₈ T _{mean}	0.56** (0.46**)	0.29* (0.20)	0.86 (0.74)
P ₈ -C ₇ T _{mean}	0.55** (0.47**)	0.25 (0.21)	0.86 (0.74)
P ₇ -C ₆ T _{mean}	0.53** (0.46**)	0.18 (0.18)	0.85 (0.73)
P ₁ -1 ₂ T _{mean}	0.61** (0.58**)	0.24 (0.37**)	0.84 (0.62)
P ₉ -C ₃ T _{max}	0.50** (0.50**)	0.23 (0.23)	0.82 (0.71)
C ₄ -C ₅ T _{max}	-0.04 (-0.12)	-0.02 (-0.08)	0.43 (0.29)
P ₁ -1 ₂ T _{max}	0.49** (0.50**)	0.09 (0.24)	0.81 (0.67)
P ₉ -C ₃ T _{min}	0.59** (0.45**)	0.42** (0.29*)	0.65 (0.41)
P ₁₀ -C ₉ T _{min}	0.59** (0.44**)	0.38** (0.25)	0.80 (0.63)
P ₉ -C ₈ T _{min}	0.59** (0.45**)	0.42** (0.29*)	0.80 (0.64)
P ₈ -C ₇ T _{min}	0.59** (0.48**)	0.42** (0.35*)	0.79 (0.64)
P ₇ -C ₆ T _{min}	0.58** (0.48**)	0.38** (0.35*)	0.79 (0.64)
P ₁ -1 ₂ T _{min}	0.64** (0.57**)	0.43** (0.48**)	0.81 (0.66)
C ₅ -C ₉ Pre	0.42** (0.45**)	0.24 (0.22)	0.39 (0.61)
P ₇ -C ₆ Pre	0.46** (0.57**)	0.42** (0.44**)	0.37 (0.64)

** Means correlation is significant at the 0.01 level; * means correlation is significant at the 0.05 level. Test of the significance was produced by the 2-tailed method. The significance testing of the 5-year smoothed series was based on the adjusted degree of freedom described by Bretherton et al. (1999)

series for the past five decades. Wang et al. (2013) also selected annual mean temperature of the previous year (January–December) as the reconstructed variable on the southeastern TP. On the other hand, climatic conditions of the previous year may precondition physiological processes within the tree and thus strongly influence the current years' tree growth (Bradley 1985). Fritts (1976) stated that in a particular region or site, the statistical calibration model may include growth predictors which lag one or more years behind the climatic occurrence, since there is sometimes a lag of growth for one or more years behind the occurrence of certain climatic variables. This statement was verified here by the autocorrelation of 0.56 in our higher elevation tree-ring series (Table 1). Further, choosing the entire calendar year is of great practical meteorological benefit (Wang et al. 2013).

3.4 Reconstruction of mean annual minimum temperature

Based on the aforementioned results, a linear transfer function ($T_{\min} = 2.72 \times \text{STD} - 11.14$) was estimated using the prior annual minimum temperature as the dependent variable and the higher forest belt chronology as the independent variable. This regression model accounts for 40 % ($r_{\text{adj}}^2 = 39.2\%$, $p < 0.001$) of the actual temperature variance over the instrumental period 1957–2010.

The split-calibration and verification statistic results presented in Table 3 give further evidence for the validity of the reconstructed model. Besides, the RE result from the leave-one-out validation indicates that there are no significant changes in correlation coefficients after any one-year value is removed from the whole time series. Further statistical results (not presented) from the first-order difference series of tree-ring chronology and minimum temperature data also support the regression function. Non-parameter results of the ST and Pmt all exceed the 95 % confidence level. This confirms that the regressed model captures both the high- and low-frequency variability.

Based on the above well calibrated and verified model, the annual minimum temperature from previous January to December was reconstructed over the full period (Fig. 6). Since the reliable chronology begins at the year 1395, we suggest some caution before that point year. The mean annual T_{\min} is -8.44 °C and the standard deviation (SD) is 0.54 °C over the full reliable period. The reconstructed T_{\min} series for the past 616 years shows decadal to multidecadal fluctuations punctuated with cool and warm periods. Herein, we define a cold (warm) period, after smoothing with an 11-year moving average, as the time span where minimum temperature values fall below (above) the long-term mean, continuously for more than 10 years. Hence, cold periods prevailed during AD 1443–1488, 1571–1614, 1621–1705, 1712–1722, 1740–1756, 1815–1824, 1913–1935

Table 3 Statistical results based on the calibration and verification of different periods for the tree-ring reconstructions of annual minimum temperature

	Calibration (1957–1985)	Verification (1986–2010)	Calibration (1983–2010)	Verification (1957–1982)	Calibration (1957–2010)
r	0.63**	0.62**	0.65**	0.61**	0.64 (0.62 ^L) **
R ²	0.40	0.39	0.42	0.37	0.40 (0.38 ^L)
R _{adj} ²	0.38	0.36	0.40	0.34	0.39 (0.37 ^L)
F	17.22**	14.76**	19.08**	13.49**	34.55 (31.48 ^L)**
RE		0.21		0.25	0.38 ^L
CE		0.12		0.11	
ST (ST ⁻¹)					38/15** (34/18*)
Pmt (Pmt ⁻¹)					3.96 ** (5.74**)

r Correlation coefficient, R² explained variance of the regression model, R_{adj}² adjusted explained variance of the regression model, RE reduction of error, CE coefficient of efficiency, ST (ST⁻¹) sign test between original (the mean of their first-order difference) observation and reconstruction series, Pmt (Pmt⁻¹) product mean test between original (departures from mean of the first-order difference) observation and reconstruction series, ** Significant at the 0.01 level, * Significant at the 0.05 level. The superscript L indicates the value is calculated from the leave-one-out method

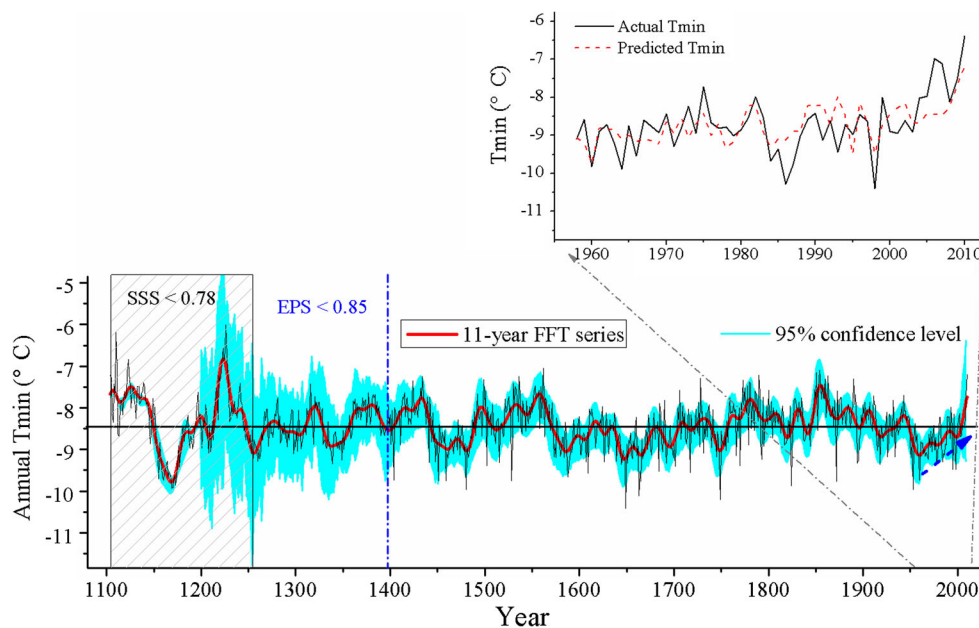


Fig. 6 Reconstructed annual (*black thin lines*) minimum temperatures from previous January to December over the full period AD 1104–2010 and the 11-year running mean series (*red heavy line*). The inserted coordinate is the detailed comparison between actual (*black solid line*) and reconstructed (*red dotted line*) minimum temperature during the common period 1957–2010. The shaded cyan area is the 95 % confidence level for the reconstructed series, including

bootstrapped error bars of the original standard tree-ring chronology (Efron 1987) and the regressed errors. The horizontal straight line is the mean minimum temperature value over the full reconstructed period. The *blue dash-dotted line* indicates the start year (1395) with $EPS > 0.85$, while the rectangle with *gray oblique lines* denotes $SSS < 0.78$. The *heavy blue arrow* indicates recent warming trend

and 1948–2003; while warm intervals occurred in AD 1407–1442, 1489–1506, 1517–1570, 1723–1734, 1757–1814, 1825–1838, 1844–1897, 1900–1912 and 1936–1947. On multidecadal to centennial scales, the most significant feature for the reconstructed temperature history is the longer cold period, which probably started from the second half of the sixteenth century and ended at the middle of the

eighteenth century. Afterwards, a comparable warm phase was predominant for about 150 years, although with two (1815–1824 and 1839–1843) short cold periods interspersed. Interestingly, the twentieth century could be defined as a cold period except for a warm interval (1936–1947). Consequently, the reconstruction gives a new perspective on recent so-called “climate warming” in a longer-term context.

4 Discussion and conclusions

4.1 Altitudinal effect

Comparison of the relationships between the two altitudinal chronologies and climate data indicates that an elevation effect probably exists in the study region, although the relative elevation is only about 200 m from the higher to the lower belt. Previous studies have generally stressed tree growth is more sensitive to temperature at its upper distribution limit while it is sensitive to drought stress at its lower limit (Fritts et al. 1965; LaMarche 1974). Salzer et al. (2009) suggested that the multi-millennial bristlecone pine ring-width series at the upper forest border was a potentially valuable resource for information regarding past temperature variability in western North America. A considerable body of further research in different climate regions (Savva et al. 2006; Yu et al. 2006; Dang et al. 2012) has confirmed such generalized tree growth-climate relationships. Although some other environmental conditions, such as snow cover, soil temperatures, soil moisture, nutrient availability and nutrient uptake, need to be taken into account when interpreting tree growth-climate relationships (Tranquilini 1979), we might expect that low temperatures limit tree growth at the upper treeline (Körner and Paulsen 2004). It is generally accepted that with increased altitude, air temperature decreases and precipitation increases (Wang et al. 2005a), which is probably applicable to the present study region as indicated from the nearest meteorological stations: Qumalai (34.13°N, 95.78°E, 4,175 m) and Qingshuihe (33.80°N, 97.13°E, 4,415 m). The mean annual temperatures over the common available period 1957–2010 are -2.09 °C and -4.56 °C, while the mean annual precipitations are 409 mm and 513 mm, respectively. Savva et al. (2006) considered that the changed relationships along altitudinal patterns may result from a combination of environmental factors representing controls on tree growth as well as differences in the length of the growing season at different elevations. Hence, the detected discrepancies of the low-frequency variability between the two altitudinal chronologies for the past 600 years are probably driven by the different climatic signals contained in each series. Consequently, we state that in such cold and arid climate region, there probably exist altitudinal effect for tree growth and propose more caution while reconstructing climate based on tree-ring series from the mountainous area.

4.2 Verification of the detected temperature signal

On the southeastern TP, the seasonal radial growth of young and old Smith fir trees was investigated by microcores collected at weekly intervals during two growing

seasons (the years 2006 and 2007) (Li et al. 2013). Consequently, both young and old trees responded to changes of the minimum air temperature, giving us the direct monitoring evidence to reconstruct local minimum temperature with tree-ring width data. To investigate whether the higher belt tree-ring chronology contains a robust temperature signal, we calculated correlations with the first principle component (PC1) series derived from 63 instrumental data on the TP (TP; Fig. 1) over the common period 1963–2010. The resulted significant ($p = 0.01$) correlation of 0.50 confirms the expectation and evidence that our tree-ring chronology can be used to reflect climate change over the whole plateau region.

The higher tree-ring chronology was also compared to Qamdo regional curve standardization (RCS) based tree-ring series, which has been successfully used to reconstruct the previous year's temperature for the whole TP (Yang 2012). During the past five decades, the correlations between the two original, the first-order difference series and the 5-year averaged series are 0.54 ($p < 0.01$), 0.44 ($p < 0.01$) and 0.60 ($p < 0.10$), respectively. Herein, the detected relationship between the two series is related to regional climate, as evidenced by the correlations between recorded precipitation and temperature series from Qumalai and Qamdo during 1957–2010 of 0.01 and 0.74, respectively. On the other hand, we can also observe from spatial correlation with the Climate Research Unit (CRU) Time Series (TS) 3.10 in Fig. 7, the precipitation data from Qumalai station are spatially more heterogeneous and therefore cannot represent the Qamdo region while the temperature data portray a larger scale temperature signal even over the whole TP. Overall, the high degree of agreement with the Qamdo tree-ring series (as shown in Fig. 8) indicates that our tree-ring record represents temperature variations over a large region. We also found that the regional temperature series is consistent with Nepal temperature variability on decadal to centennial timescales (Fig. 9). The February–June temperature records recovered by Cook et al. (2003) correlated at 0.18 ($p < 0.001$) with our presented temperature series over the common period AD 1546–1991. The correlation increased to 0.31 after the 11-year smoothed series was compared.

4.3 Recent warming trend in the context of the past 600 years

Recent warming trend during the past five decades (1948–2003) was identified as a cold period in the context of the past 600 years (Fig. 6). The cold interval of the past 50 years is comparable to those of any comparable period over the past 600 years, including the coldest periods of the Little Ice Age. Similarly, in the western Nepal, Sano et al. (2005) also detected a notable March–September cold

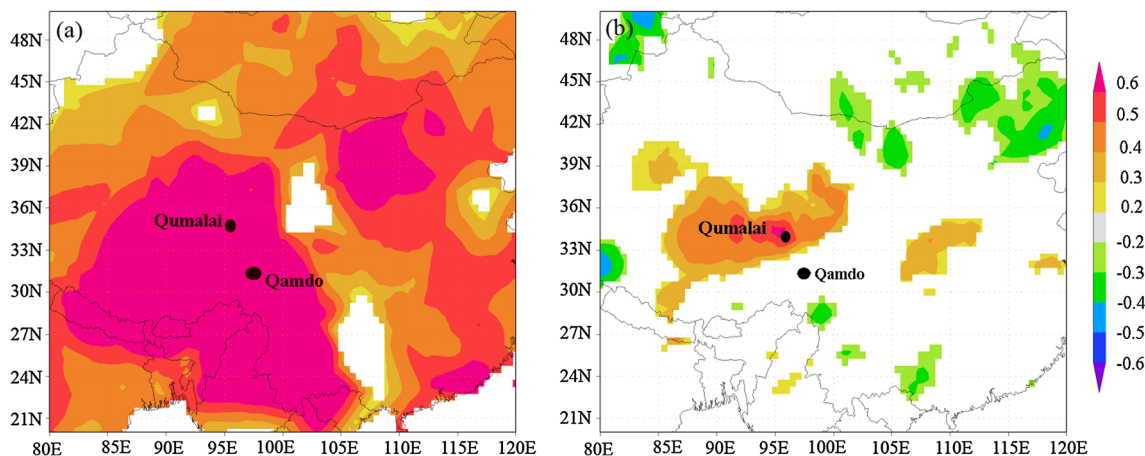


Fig. 7 Spatial correlations of temperature **a** and precipitation **b** recorded from Qumalai station with the gridded Climatic Research Unit (CRU) Time Series (TS) 3.1 annual (January–December) temperature and the gridded annual precipitation signal

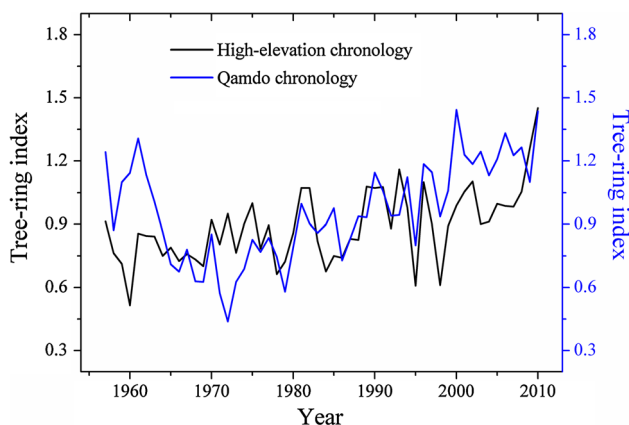


Fig. 8 Comparison between the presented high-elevation tree-ring chronology (black line) and Qamdo RCS based chronology (blue line) during the past five decades

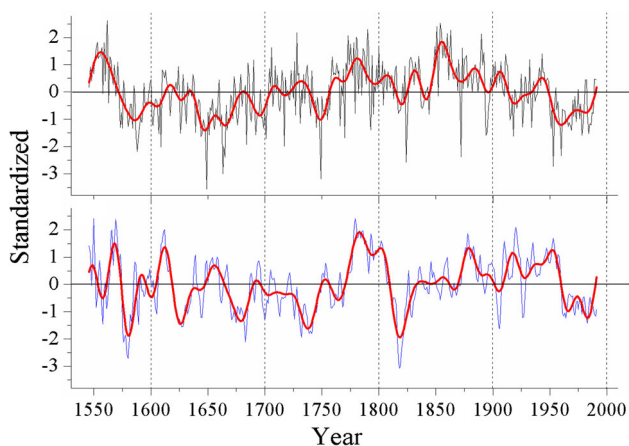


Fig. 9 Comparison between our presented annual minimum temperature (the upper gray line) and Nepal February–June temperature series (the lower blue line), Cook et al. (2003) during the common period AD 1546–1991. Both temperature series have been standardized to facilitate comparison. The thick red lines are the corresponding 11-year low-pass filtered series

period continuing up from 1950 to 1991 and stated that a consistent warming trend over the last century or two cannot be found in their ring width and wood density of *Abies spectabilis* based reconstruction. Cook et al. (2003) found that February–June temperatures have actually cooled since 1960 in the Himalayas of Nepal. Again, both instrumental records and reconstructed data showed that March–May temperatures have decreased during the latter part of the twentieth century in Western Himalaya (Yadav and Singh 2002; Yadav et al. 2004). Similar cooling for the past decades were also recorded in other locations, such as in Karakorum Mountains of Pakistan (Esper 2000), in the Tibet and central Asia (Briffa et al. 2001), in the central Asia mountain regions (Diaz and Bradley 1997), and in the northern Yakutia of Siberia (Hughes et al. 1999). Herein, we considered that cooling during recent decades in the different study regions could be regarded as a large-scale climatic fluctuation.

4.4 Comparison with other temperature series

Compared to the summer (May–July) mean temperature variability derived from stable carbon isotope ($\delta^{13}\text{C}$) series (Xu et al. 2011), we found the common warm period of 1936–1948 and common cold period of 1913–1935, which correspond to the advance or stability of the Lhamcoka glacier in the Chola Shan mountains (Bräuning and Griebinger 2006) and rapid glacier retreat in the Gongga mountain (Li and Su 1996), respectively. Both the two temperature series detected a common warming trend during the past two decades, in accordance with the accelerated glacial retreat rates after the 1980s (He et al. 2003; Li et al. 2010).

By simply standardizing six warm season temperature-sensitive records (Shao and Fan 1999; Gou et al. 2007; Liang et al. 2008; Fan et al. 2009, 2010; Li et al. 2012) over

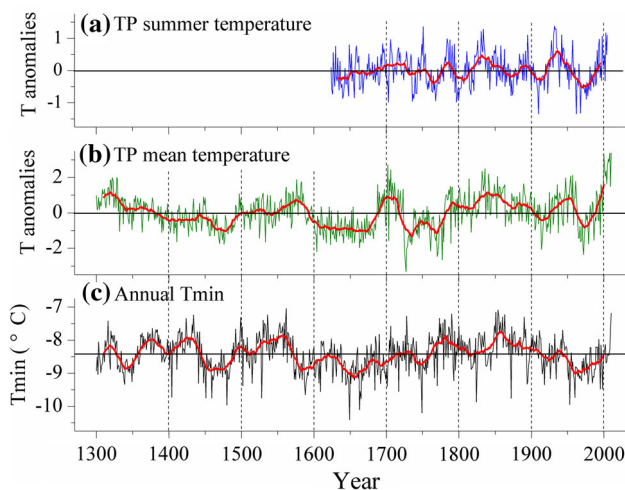


Fig. 10 Comparisons between reconstructed summer (March–August) temperature series by Yang (2012) (a, blue line), TP mean temperature series inferred from Qamdo tree-ring series (b, green line) and annual minimum temperature series in this study (c, black line) over their common periods. The thick red lines are the corresponding 21-year averaged series. The horizontal black lines are the averaged levels for the associated temperature series

the common period AD 1624–2005, Yang (2012) composited a warm season (March–August) temperature series (Fig. 10a) to reflect summer temperature variability over the whole TP. Compared to our reconstruction (Fig. 10c), we found consistent increasing or decreasing trend between the two series, although with different amplitudes. Furthermore, Qamdo RCS based temperature series (Fig. 10b), which is verified to represent the prior year annual temperature variability for whole TP region (Yang 2012; Wang et al. 2013), correlates at 0.31 and 0.36 with the presented new original record and the first-order difference series over their common reliable period AD 1395–2010. Such significant ($p < 0.001$) correlations indicate the coherent variability of the two series. Similar warm/cold periods on the interdecadal to multidecadal scales can also be identified with other reconstructions (Bräuning and Mantwill 2004; Liang et al. 2009; Yang et al. 2010; Wang et al. 2013).

We further compared our annual temperature reconstruction with the northern hemispheric temperature reconstructions of Esper et al. (2002), Moberg et al. (2005) and Christiansen and Ljungqvist (2012) over their common reliable periods of AD 1395–1992, AD 1395–1979 and AD 1395–1973, respectively. The correlation coefficients between central TP temperature and northern hemisphere temperature data during their common periods are 0.13, 0.14 and 0.12, respectively. However, before the middle of the nineteenth century (the point year AD 1850), the corresponding correlations are 0.36, 0.23 and 0.33, while after that, the relationship significantly reversed, with the

associated correlations of -0.50 , -0.24 and -0.45 , respectively. All the aforementioned correlations are significant at the 0.05 level. After 11-year smoothed series were used, the correlations during AD 1395–1850 and the last ~ 150 years increased to 0.59 and -0.74 with Esper et al. (2002) reconstruction, 0.43 and -0.52 with the Moberg et al. (2005) reconstruction and 0.59 and -0.66 with the Christiansen and Ljungqvist (2012) reconstruction. Thus, we state that, from the end of the fourteenth century to the middle of the nineteenth century, the variability of central TP temperature is in phase with the northern hemispheric temperature. Thereafter, out of phase fluctuations can be identified, which could be due to the regional factors: these need examination by more detailed research. On the other hand, the varying seasonality and different factors (maximum, minimum and average temperature) recovered may cause some bias. Consequently, we propose that more detailed regional climate records, especially in some of the mountainous regions, are needed to better understand large scale spatiotemporal fingerprints of climatic change (e.g., Esper et al. 2002; Mann et al. 2009) in the future. Anyhow, the coherence recorded before the middle of the nineteenth century temperature variations in the two series (central TP temperature and the Northern Hemispheric temperature) could reflect the similar mechanisms that drive the multidecadal to centennial temperature variations, also suggesting that the multidecadal synchronous changes are robust results.

Overall, despite the times of the beginning and ending of change phases differing somewhat, and the observed differences in the magnitudes of fluctuations, the present new series shows similar variations in warm or cold phases to the other temperature related records. The associated discrepancies may be related to (1) the different sampling sites as well as local microclimate context; (2) the use of different (target) instrumental data and the differing calibration periods; (3) perhaps slightly differing seasonalities (Frank and Esper 2005), making an estimation of the long-term absolute temperature amplitude inconclusive; and (4) inconsistent variability between the mean, maximum and minimum temperatures as also suggested by Wilson and Luckman (2002, 2003). Hence, the existence of such detailed differences over the various geographic regions warrants the need to develop more and longer data sets to achieve an accurate hemispheric view of climate change.

4.5 Correlations with the Asian summer monsoon strength

Wang et al. (2005b) established a 5-year-resolution absolute-dated speleothem $\delta^{18}\text{O}$ -record from Dongge Cave (Fig. 11c), southern China, which provides a continuous

history of the Asian summer monsoon variability. Burns et al. (2002) developed an annually resolved record of Indian monsoon rainfall variation for the past 780 years based on annual layer thickness and stable isotope ($\delta^{18}\text{O}$: Fig. 11d) analyses of a laminated stalagmite from southern Oman. On the decadal and multidecadal scales, the correlation coefficients between our central TP temperature series and the $\delta^{18}\text{O}$ chronology from the Dongge cave are -0.31 ($n = 60$) initially and -0.34 after 3-year averaged series, respectively. The correlation with the $\delta^{18}\text{O}$ series from the Oman cave is weaker ($r = -0.01$); however, we detected that the correlations with the $\delta^{13}\text{C}$ series from the Oman cave are higher, with -0.26 and -0.33 for the associated original and 3-year smoothed series. Burns et al. (2002) stated that both $\delta^{18}\text{O}$ and $\delta^{13}\text{C}$ values vary primarily in response to changes in the amount of precipitation, although controlled by different mechanisms. Furthermore, considering the Dongge Cave $\delta^{18}\text{O}$ chronology was established by ^{230}Th dates with an age uncertainty of 50 years, we smoothed all the series with a 50-year FFT (Fast Fourier Transform) function to facilitate the comparison. From Fig. 11 we are confident that warmer temperature over the TP is associated with strong Asian summer monsoon, while colder conditions are related to weak monsoon trends. That is to say, the thermal conditions over the TP have an important influence on the strength of the Asian summer monsoon on multidecadal to centennial timescales. With two short warm period fluctuations over the central region, temperatures over the whole TP can be identified as a colder condition from fifteenth century to the middle of the eighteenth century,

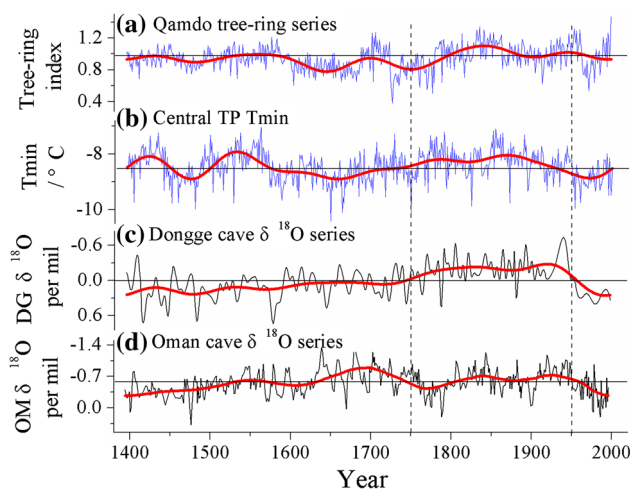


Fig. 11 Associations between temperature series over the whole TP (a), central TP (b), and Asian monsoon strength inferred from Dongge cave (c, DG) and Oman cave (d, OM) $\delta^{18}\text{O}$ series over the full reliable period AD 1395–2010. The thick red lines are the corresponding 50-year FFT series, while the horizontal black lines are the average levels for the four series, respectively

which is accompanied by the weakened Asian summer monsoon (Fig. 11). Afterwards, an increasing warming trend and also strengthened monsoon signal can be detected until the middle of the twentieth century. For the past 50 years, colder climate and weakened monsoon prevailed. Burns et al. (2002) stressed that over most of the twentieth century monsoon rainfall was decreasing. They considered that such weakened monsoon intensity was a response to the warming of the Indian Ocean during the twentieth century. From our results, we speculate that the decreasing temperature over the TP may also have contributed to the weakened monsoon rainfall. The cold surface temperature on the TP may create a weak pressure gradient between the TP and the Indian Ocean, resulting in weakened Asian summer monsoon (Fleitmann et al. 2007), and vice versa. Such detailed mechanisms have been thoroughly elaborated by Yang et al. (2007). Anyhow, the detected teleconnections remain to be explained further by modeling and investigation of more sensitive and high-resolution climate proxy records in the future.

To sum up, our results show that juniper tree-ring width chronology in the higher elevation belt at the cold and arid central TP region is mainly induced by regional annual minimum temperature variability, while tree growth in the lower elevation belt may contain both temperature and precipitation signals. Such results direct us to be more cautious while using tree-ring chronology to reconstruct local or regional climate history. The detected temperature signal from the higher elevation belt tree-ring width chronology was firmly verified. Based on a well calibrated and verified regression model, 600 years long annual minimum temperature history was firstly recovered for the central TP region. Specifically, the warming trend during the past five decades (1948–2003) is identified as a cool period in the context of the six century years. The recovered temperature history agrees well with other temperature series over the whole TP region, demonstrating that our reconstructed temperature could be used to evaluate regional climate change. In addition, the detected temperature variability also mirrors the northern hemispheric temperature before the middle of the nineteenth century. Moreover, we found that temperature variability on the TP plays an important role in the Asian summer monsoon circulation through its thermal effects. The continuing expansion and development of tree-ring networks in the TP will lead to large-scale reconstructions of past climate over this critically important region. The results presented here are an important step in that direction. However, considering our temperature series is 600 years long, we propose a little caution with the interpreted results and recommend a search for more older trees or other associated longer and higher-resolved proxy records, to thoroughly understand climate change in the context of thousands of years.

Acknowledgments The authors are grateful to the editor and the two anonymous reviewers for their invaluable comments. The study was jointly funded by the National Science Foundation of China (Grant No. 41272189) and the CAS Strategic Priority Research Program Grant (No. XDA05080801). Nina M. Datsenko was supported by the CAS Visiting Professorship for Senior International Scientists (Grant No. 2012T1Z0033) and the Russian Foundation for Basic Research (12-05-00049 and 09-05-00202-a). Bao Yang gratefully acknowledges the support of the K.C. Wong Education Foundation, Hong Kong.

References

- Biondi F, Waikul K (2004) DENDROCLIM2002: a C++ program for statistical calibration of climate signals in tree-ring chronologies. *Comput Geosci* 30(3):303–311
- Bradley RS (1985) Quaternary paleoclimatology: methods of paleoclimatic reconstruction. Allen and Unwin, Boston
- Bräuning A, Griebinger J (2006) Late Holocene variations in monsoon intensity in the Tibetan-Himalayan region-evidence from tree rings. *J Geol Soc India* 68(3):485–493
- Bräuning A, Mantwill B (2004) Summer temperature and summer monsoon history on the Tibetan Plateau during the last 400 years recorded by tree rings. *Geophys Res Lett* 31:L24205. doi:10.1029/2004GL020793
- Bretherton CS, Widmann M, Dymnikov VP, Wallace JM, Bladé I (1999) The effective number of spatial degrees of freedom of a time-varying field. *J Clim* 12:1990–2009
- Briffa KR (1995) Interpreting high-resolution proxy climate data: the example of dendroclimatology. In: vonStorch H, Navarra A (eds) Analysis of climate variability, applications of statistical techniques. Springer, Berlin Heidelberg New York
- Briffa KR (2000) Annual climate variability in the Holocene: interpreting the message of ancient trees. *Quat Sci Rev* 19:87–105
- Briffa KR, Osborn TJ, Schweingruber FH, Harris IC, Jones PD, Shiyatov SG, Vaganov EA (2001) Low frequency temperature variations from northern tree ring density network. *J Geophys Res* 106:2929–2941
- Briffa KR, Osborn TJ, Schweingruber FH, Jones PD, Shiyatov SG, Vaganov EA (2002) Tree-ring width and density data around the Northern Hemisphere: part 2, spatio-temporal variability and associated climate patterns. *Holocene* 12:759–789
- Briffa KR, Osborn TJ, Schweingruber FH (2004) Large-scale temperature inferences from tree rings: a review. *Glob Planet Change* 40:11–26
- Büntgen U, Esper J, Frank DC, Nicolussi K, Schmidhalter M (2005) A 1052-year tree-ring proxy for Alpine summer temperatures. *Clim Dyn* 25:141–153. doi:10.1007/s00382-005-0028-1
- Büntgen U, Frank DC, Nievergelt D, Esper J (2006) Summer temperature variations in the European Alps, A.D. 755–2004. *J Clim* 19:5606–5623
- Büntgen U, Tegel W, Nicolussi K, McCormick M, Frank D, Trouet V, Kaplan JO, Herzig F, Heussner KU, Wanner H, Luterbacher J, Esper J (2011) 2500 years of European climate variability and human susceptibility. *Science* 331:578–582. doi:10.1126/science.1197175
- Burns SJ, Fleitmann D, Mudelsee M, Neff U, Matter A, Mangini A (2002) A 780-year annually resolved record of Indian Ocean monsoon precipitation from a speleothem from south Oman. *J Geophys Res* 107:4434. doi:10.1029/2001JD001281
- Christiansen B, Ljungqvist FC (2012) The extra-tropical Northern Hemisphere temperature in the last two millennia: reconstructions of low-frequency variability. *Clim Past* 8:765–786
- Cook ER (1985) A time-series analysis approach to tree-ring standardization, PhD dissertation. The University of Arizona Press, Tucson
- Cook ER, Kairiukstis LA (1990) Methods of dendrochronology. Kluwer Academic Press, Netherlands
- Cook ER, Peters K (1997) Calculating unbiased tree-ring indices for the study of climatic and environmental change. *Holocene* 7:361–370
- Cook ER, Briffa KR, Meko DM, Graybill DA, Funkhouser G (1995) The ‘segment length curse’ in long tree-ring chronology development for palaeoclimatic studies. *Holocene* 5:229–237
- Cook ER, Krusic PJ, Jones PD (2003) Dendroclimatic signals in long tree-ring chronologies from the Himalayas of Nepal. *Int J Climatol* 23:707–732
- Cook ER, Anchukaitis KJ, Buckley BM, D’Arrigo RD, Jacoby GC, Wright WE (2010) Asian monsoon failure and megadrought during the last millennium. *Science* 328:486–489. doi:10.1126/science.1185188
- D’Arrigo R, Wilson R, Jacoby G (2006) On the long-term context for late 20th century warming. *J Geophys Res* 111:D03103
- Dang HS, Zhang YJ, Zhang KY, Jiang MX, Zhang QF (2012) Climate-growth relationships of subalpine fir (*Abies fargesii*) across the altitudinal range in the Shennongjia Mountains, central China. *Clim Change* 117(4):903–917. doi:10.1007/s10584-012-0611-5
- Diaz HF, Bradley RS (1997) Temperature variations during the last century at high elevation sites. *Clim Change* 36:253–279
- Efron B (1987) Better bootstrap confidence intervals. *J Am Stat Assoc* 82:171–185
- Esper J (2000) Long-term tree-ring variations in Juniperus at the upper timberline in the Karakorum (Pakistan). *Holocene* 10:253–260
- Esper J, Cook ER, Schweingruber FH (2002) Low-frequency signals in long chronologies for reconstructing past temperature variability. *Science* 295:2250–2253. doi:10.1126/science.1066208
- Fan ZX, Bräuning A, Yang B, Cao KF (2009) Tree ring density-based summer temperature reconstruction for the central Hengduan Mountains in southern China. *Glob Planet Change* 65:1–11
- Fan ZX, Bräuning A, Tian QH, Yang B, Cao KF (2010) Tree ring recorded May–August temperature variations since A.D. 1585 in the Gaoligong Mountains, southeastern Tibetan Plateau. *Palaeogeogr Palaeoclimatol Palaeoecol* 296:94–102
- Fleitmann D, Burns SJ, Mangini A, Mudelsee M, Kramers J, Villa I, Neff U, Al-Subbaray AA, Buettner A, Hippler D, Matter A (2007) Holocene ITCZ and Indian monsoon dynamics recorded in stalagmites from Oman and Yemen (Socotra). *Quat Sci Rev* 26:170–188
- Frank D, Esper J (2005) Temperature reconstructions and comparisons with instrumental data from a tree-ring network for the European Alps. *Int J Climatol* 25(11):1437–1454
- Fritts HC (1976) Tree rings and climate. Academic Press, London 567
- Fritts HC, Smith DG, Cardis JW, Budelsky CA (1965) Tree-ring characteristics along a vegetation gradient in northern Arizona. *Ecology* 46:393–401
- Gou XH, Chen FH, Jacoby G, Cook E, Yang MX, Peng JF, Zhang Y (2007) Rapid tree growth with respect to the last 400 years in response to climate warming, northeastern Tibetan Plateau. *Int J Climatol* 27:1497–1503
- Harsch MA, Hulme PE, McGlone MS, Duncan RP (2009) Are treelines advancing? A global meta-analysis of treeline response to climate warming. *Ecol Lett* 12:1040–1049
- He YQ, Zhang ZL, Theakstone WH, Chen T, Yao TD, Pang HX (2003) Changing features of the climate and glaciers in China’s monsoonal temperate glacier region. *J Geophys Res* 108:4530–4536. doi:10.1029/2002JD003365
- Holmes RL (1983) Computer-assisted quality control in tree-ring dating and measurement. *Tree-Ring Bull* 43:69–95

- Hughes MK, Vaganov EA, Shiyatov S, Touchan R, Funkhouser G (1999) Twentieth century summer warmth in northern Yakutia in a 600-year context. *Holocene* 9:629–634
- Jin LY, Qin NS, Gou XH, Chen FH, Li J (2005) Series of spring maximum temperature in southern Qinghai plateau and analysis of its variations during the last 450 years. *Quat Sci* 25(2): 193–201 in Chinese, with English abstract
- Jones PD, Briffa KR, Osborn TJ, Lough JM, van Ommen TD, Vinther BM, Luterbacher J, Wahl ER, Zwiers FW, Mann ME, Schmidt GA, Ammann CM, Buckley BM, Cobb KM, Esper J, Goosse H, Graham N, Jansen E, Kiefer T, Kull C, Küttel M, Mosley-Thompson E, Overpeck JT, Riedwyl N, Schulz M, Tudhope AW, Villalba R, Wanner H, Wolff E, Xoplaki E (2009) High-resolution palaeoclimatology of the last millennium: a review of current status and future prospects. *Holocene* 19:3–49
- Körner C, Paulsen J (2004) A world-wide study of high altitude treeline temperatures. *J Biogeogr* 31:713–732
- LaMarche VJ (1974) Paleoclimatic inferences inferred from long tree ring records. *Science* 183(4129):1043–1048
- Li JJ, Su Z (1996) *Glaciers in the Hengduan Mountains* (in Chinese). Science, Beijing
- Li ZX, He YQ, Pu T, Jia WX, He XZ, Pang HX, Zhang NN, Liu Q, Wang SJ, Zhu GF, Wang SX, Chang L, Du JK, Xin HJ (2010) Changes of climate, glaciers and runoff in China's monsoonal temperate glacier region during the last several decades. *Quaternary International* 218:13–28. doi:10.1016/j.quaint.2009.05.010
- Li ZS, Zhang QB, and Ma K (2012) Tree-ring reconstruction of summer temperature for A.D. 1475–2003 in the central Hengduan Mountains, Northwestern Yunnan, China. *Clim Change* 110 (1–2): 455–467. doi:10.1007/s10584-011-0111-z
- Li XX, Liang EY, Gričar J, Prislán P, Rossi S, Čufar K (2013) Age dependence of xylogenesis and its climatic sensitivity in Smith fir on the south-eastern Tibetan Plateau. *Tree Physiol* 33:48–56. doi:10.1093/treephys/tps113
- Liang EY, Shao XM, Qin NS (2008) Tree-ring based summer temperature reconstruction for the source region of the Yangtze River on the Tibetan Plateau. *Global Planet Change* 61(3–4): 313–320
- Liang EY, Shao XM, Xu Y (2009) Tree-ring evidence of recent abnormal warming on the southeast Tibetan Plateau. *Theor Appl Climatol* 98(1–2):9–18
- Liang EY, Wang YF, Eckstein D, Luo TX (2011) Little change in the fir tree-line position on the southeastern Tibetan Plateau after 200 years of warming. *New Phytol* 190(3):760–769
- Liu XD, Chen BD (2000) Climatic warming in the Tibetan Plateau during recent decades. *Int J Climatol* 20:1729–1742
- Luterbacher J, Dietrich D, Xoplaki E, Grosjean M, Wanner H (2004) European seasonal and annual temperature variability, trends, and extremes since 1500. *Science* 303:1499–1503
- Mann ME, Lees J (1996) Robust estimation of background noise and signal detection in climatic time series. *Clim Change* 33:409–445
- Mann ME, Zhang Z, Rutherford S, Bradley RS, Hughes MK, Shindell D, Ammann C, Faluvegi G, Ni F (2009) Global signatures and dynamical origins of the Little Ice Age and Medieval Climate Anomaly. *Science* 326:1256–1260
- Meko DM, Graybill DA (1995) Tree-ring reconstruction of upper Gila River discharge. *Water Resource Bulletin* 31:605–616
- Michaelsen J (1987) Cross-validation in statistical climate forecast models. *J Clim Appl Meteorol* 26:1589–1600
- Moberg A, Sonechkin DM, Holmgren K, Datsenko NM, Karlen W (2005) Highly variable Northern Hemisphere temperatures reconstructed from low- and high-resolution proxy data. *Nature* 433:613–617
- Osborn TJ, Briffa KR, Jones PD (1997) Adjusting variance for sample size in tree-ring chronologies and other regional mean time series. *Dendrochronologia* 15:89–99
- Rinn F (2003) *TSAPWin: Time series analysis and presentation for dendrochronology and related applications*. Version 0.55 User reference, Heidelberg, p 76
- Salzer MW, Hughes MK, Bunn AG, Kipfmüller KF (2009) Recent unprecedented tree-ring growth in bristlecone pine at the highest elevations and possible causes. *Proc Natl Acad Sci USA* 106(48):20348–20353
- Sano M, Furuta F, Kobayashi O, Sweda T (2005) Temperature variations since the mid-18th century for western Nepal, as reconstructed from tree-ring width and density of *Abies spectabilis*. *Dendrochronologia* 23:83–92
- Savva Y, Oleksyn J, Reich PB, Tjoelker MG, Vaganov EA, Modrzyński J (2006) Interannual growth response of Norway spruce to climate along an altitudinal gradient in the Tatra Mountains, Poland. *Trees* 20:735–746
- Shao XM, Fan JM (1999) Past climate on west Sichun Plateau as reconstructed from ring-width of Dragon spruce. *Quat Sci* 1:81–89
- Stokes MA, Smiley TL (1968) *An introduction to tree-ring dating*. The University of Chicago Press, Chicago, p 73
- Tranquillini W (1979) *Physiological Ecology of the Alpine Timberline. Tree Existence at High Altitudes with Special References to the European Alps*. Ecological Studies 31. Springer Verlag, Berlin
- Wang T, Ren HB, Ma KP (2005a) Climatic signals in tree ring of *Picea schrenkiana* along an altitudinal gradient in the central Tianshan Mountains, northwestern China. *Trees* 19:735–741
- Wang YJ, Cheng H, Edwards RL, He YQ, Kong XG, An ZS, Wu JY, Kelly MJ, Dykoski CA, Li XD (2005b) The Holocene Asian monsoon, links to solar changes and North Atlantic climate. *Science* 308:854–857. doi:10.1126/science.1106296
- Wang NL, Xi Jiang, Thompson LG, Davis ME (2007) Accumulation rates over the past 500 years recorded in ice cores from the northern and southern Tibetan Plateau, China. *Arct Antarct Alp Res* 39(4):671–677
- Wang JL, Yang B, Qin C, Kang SY, He MH, Wang ZY (2013) Tree-ring inferred annual mean temperature variations on the southeastern Tibetan Plateau during the last millennium and their relationships with the Atlantic Multidecadal Oscillation. *Clim Dyn*. doi:10.1007/s00382-013-1802-0
- Wigley T, Briffa KR, Jones PD (1984) On the average value of correlated time series, with applications in dendroclimatology and hydrometeorology. *J Clim Appl Meteorol* 23:201–213
- Wilson RJS, Luckman BH (2002) Tree-ring reconstruction of maximum and minimum temperatures and the diurnal temperature range in British Columbia, Canada. *Dendrochronologia* 20(3):257–268
- Wilson RJS, Luckman BH (2003) Dendroclimatic reconstruction of maximum summer temperatures from upper treeline sites in Interior British Columbia, Canada. *Holocene* 13:851–861
- Xu GB, Chen T, Liu XH, Jin LY, An WL, Wang WZ (2011) Summer temperature variations recorded in tree-ring $\delta^{13}\text{C}$ values on the northeastern Tibetan Plateau. *Theor Appl Climatol* 105:51–63
- Yadav RR, Singh J (2002) Tree-ring-based spring temperature patterns over the past four centuries in Western Himalaya. *Quat Res* 57:299–305
- Yadav RR, Park WK, Singh J, Dubey B (2004) Do the western Himalayas defy global warming? *Geophys Res Lett* 31:L17201. doi:10.1029/2004GL020201
- Yang B (2012) Spatial and temporal patterns of climate variations over the Tibetan Plateau during the period 1300–2010. *Quat Sci* 32 1:81–94 (in Chinese, English abstract)

- Yang B, Bräuning A, Yao TD, Davis ME (2007) Correlation between the oxygen isotope record from Dasuopu ice core and the Asian Southwest Monsoon during the last millennium. *Quat Sci Rev* 26:1810–1817
- Yang B, Kang XC, Bräuning A, Liu JJ (2010) A 622-year regional temperature history of southeast Tibet derived from tree rings. *Holocene* 20(2):181–190
- Yang B, Qin C, Shi F, Sonechkin DM (2012a) Tree ring-based annual streamflow reconstruction for the Heihe River of arid north-western China since AD 575 and its implication to water resources management. *Holocene* 21(7):773–784
- Yang B, Sonechkin DM, Datsenko NM, Ivashchenko NN, Liu J, Qin C (2012b) The eigen analysis of tree-ring records: part 3, taking heteroscedasticity and sampling effects into consideration. *Theoret Appl Climatol* 107(3–4):519–530
- Yu DP, Wang QL, Wang GG, Dai LM (2006) Dendroclimatic response of *Picea jezoensis* along an altitudinal gradient in Changbai Mountains. *Sci China Ser E* 49:150–159
- Zhang YX, Shao XM, Wilmking M (2011) Dynamic relationships between *Picea crassifolia* growth and climate at upper treeline in the Qilian Mts., Northeast Tibetan Plateau, China. *Dendrochronologia* 29:185–199
- Zhu HF, Shao XM, Yin ZY, Xu P, Xu Y, Tian H (2011) August temperature variability in the southeastern Tibetan Plateau since AD 1385 inferred from tree rings. *Palaeogeogr Palaeoclimatol* 305(1–4):84–92